DOI: 10.1002/ejic.201100350

Crystal Structure and Properties of $Yb_5Ni_4Ge_{10}$

Sebastian C. Peter,[a,b] Sudhindra Rayaprol,[c] Melanie C. Francisco,[a] and Mercouri G. Kanatzidis*[a]

Dedicated to Professor John D. Corbett on the occasion of his 85th birthday

Keywords: Rare earths / Intermetallic phases / Magnetic properties / Heat capacity / Ytterbium

The new compound $Yb_5Ni_4Ge_{10}$ was obtained as single crystals in high yield from reactions run in liquid indium. Single-crystal X-ray diffraction data showed that it crystallizes in the $Sc_5Co_4Si_{10}$ structure type in the tetragonal space group *P*4/*mbm*. The structure is a three-dimensional framework of $[Ni_4Ge_{10}]$ atoms with voids filled by Yb atoms. The Ni and Ge atoms form pentagons, hexagons, and octagons along the *ab* one-dimensional plane, which are interconnected along the *c* axis via Ni–Ge–Ni zigzag chains. Magnetic measurements reveal that $Yb_5Ni_4Ge_{10}$ crystals show paramagnetic behavior with a lack of long-range magnetic ordering down to 2 K. The magnetic susceptibility deviates from the Curie–Weiss law below 100 K, presumably because of crystal field effects from Yb^{3+} ions. In specific heat measurements, the compound exhibits non-Fermi-liquid-like behavior at low temperatures.

Introduction

Ternary intermetallic compounds $RE_5T_4X_{10}$ (RE = rare earth, T = Co, Rh, Ir, Os, X = Si, Ge, Sn) crystallize in the tetragonal $Sc_5Co_4Si_{10}$ type structure,[1] in which the rare earth atoms occupy three non-equivalent crystallographic positions. These compounds exhibit unusual magnetic and superconducting properties with a charge density wave (CDW) transition.[2] $RE_5Rh_4Sn_{10}$ (RE = Ce, Pr, Nd) show magnetic ordering at 4.3, 5.6, and 7.3 K for Ce, Pr, and Nd analogs, respectively.[3] Magnetic and specific heat data indicate that $RE_5Rh_4Ge_{10}$ (RE = Gd, Tb, Dy, Ho, Er, Tm) are antiferromagnetic with Néel temperatures equal to 11.5 (RE = Tb), 6.2 (RE = Dy), 6.3 (RE = Ho), 5.6 (RE = Er), and 6.9 K (RE = Tm).[4] The $RE_5T_4X_{10}$ (RE = Sc, Y, and Lu; T = Co, Rh, Ir, and Os; X = Si and Ge) compounds were reported as superconductors at low temperatures.[5,6]

Among the trivalent rare earth compounds, the Yb-based intermetallics, which are considered as the hole counterparts to the isostructural cerium compounds (i.e. f^{13} vs. f^1 systems), have received considerable attention for the past few years. This interest originates from the ability of Yb to exhibit various peculiar properties such as intermediate-valence, heavy fermion, or Kondo behavior and unusual magnetism.[7–9] These properties are generally believed to arise from the strong hybridization (interaction) between the localized 4f electrons and the delocalized s, p, d conduction electrons.[10,11] So far, several ytterbium compounds, $Yb_5T_4X_{10}$ (T = Co, Rh, Ir and X = Si, Ge) within the $Sc_5Co_4Si_{10}$ type structure have been reported.[12,13] Magnetic and transport studies on $Yb_5T_4Ge_{10}$ (T = Co, Rh, Ir) show that they are paramagnetic metals.[12] Coexistence of magnetic ordering (antiferromagnetic at 50 K) and a charge density wave was observed in $Yb_5Ir_4Si_{10}$.[13]

Within the $Sc_5Co_4Si_{10}$ type, no compounds have been reported with Ni as the transition element. One motivation for the work described here is the continued development of the intermetallic chemistry of Yb[14–21] and the deeper understanding of the ability of Yb to adopt different or mixed oxidation states. There are a few compounds reported within the Yb–Ni–Ge system. The first compound discovered was $YbNi_2Ge_2$, a $ThCr_2Si_2$ type reported in 1959 by Rieger et al.[22] Later, the crystal structure and magnetic properties of YbNiGe, a TiNiSi type structure, was studied by Gorelenko et al.[23] In 1983, Dzyanyi et al. reported a series of compounds, $YbNi_{4.4}Ge_{0.6}$, $YbNi_{0.25}Ge_{1.75}$, $YbNiGe_2$, $YbNiGe_3$, $YbNi_5Ge_3$, $Yb_2Ni_{15.1}Ge_{1.9}$, Yb_2NiGe_6, and $Yb_3Ni_{11}Ge_4$, and they proposed the phase diagram of the Yb–Ni–Ge system for the first time.[24] $YbNi_5Ge_3$ orders antiferromagnetically at 2.7 K.[25] Magnetic and transport properties of Yb_2NiGe_6 and $YbNiGe_3$ were studied in detail.[26–28] Recently, we reported the synthesis of $YbNiGe_2$ using In as a metallic flux.[29] $YbNiGe_2$ crystallizes in the orthorhombic *Immm* space group and possesses the $YIrGe_2$ structure type.

[a] Department of Chemistry, Northwestern University, Evanston, IL 60208, USA
E-mail: m-kanatzidis@northwestern.edu
[b] New Chemistry Unit, Jawaharlal Nehru Centre for Advanced Scientific Research, Jakkur, Bangalore 560064, India
[c] UGC-DAE Consortium for Scientific Research, Mumbai Centre, BARC, R-5 Shed, Trombay, Mumbai 400085, India

During our phase investigations of the Yb–Ni–Ge system, we used liquid indium as flux medium as a convenient and powerful tool in exploring new phases.[30] In this paper, we report the new compound $Yb_5Ni_4Ge_{10}$ with the $Sc_5Co_4Si_{10}$ type structure. The synthesis and crystal structure as well as magnetization and heat capacity data for $Yb_5Ni_4Ge_{10}$ are presented.

Results and Discussion

Reaction Chemistry

$Yb_5Ni_4Ge_{10}$ was obtained from Yb/Ni/Ge reactions in liquid In, from which the new tetragonal phase was isolated in high yield (>95%). The light gray rod-shaped single crystals up to 5 mm in length were stable in air, and no decomposition was observed even after several months. SEM images of typical rod-like crystals of $Yb_5Ni_4Ge_{10}$ as grown from the flux synthesis are shown in Figure 1. Other synthetic techniques such as arc melting, high-frequency induction heating, or direct heating in resistive furnaces were not successful in producing the title compound.

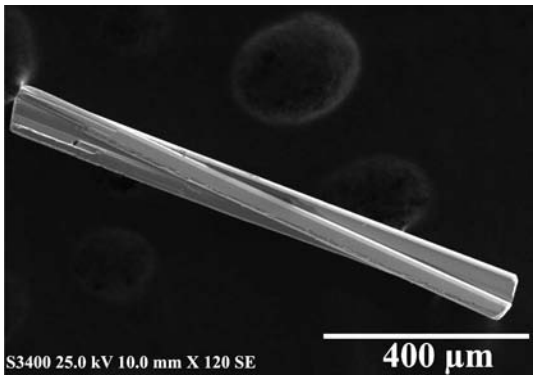

Figure 1. SEM image of two overlapping typical single crystals of $Yb_5Ni_4Ge_{10}$.

Crystal Chemistry

A projection of the $Yb_5Ni_4Ge_{10}$ structure is shown in Figure 2A. $Yb_5Ni_4Ge_{10}$ crystallizes in a primitive tetragonal lattice (*P*4/*mbm*) of $Sc_5Co_4Si_{10}$ type structure. The $Yb_5Ni_4Ge_{10}$ compound is composed of a complex $[Ni_4Ge_{10}]^{3-}$ polyanion network with three types of one-dimensional channels, propagating along the *c* axis, in which the ytterbium ions are embedded.

The pentagonal channels are formed by $[Ni_2Ge_3]$ five-membered rings, which are interconnected along the *c* axis by Ni–Ge3–Ni zigzag chains. Yb2 atoms are sandwiched between the pentagonal rings. The second tunnel is based on planar $[Ni_2Ge_4]$ hexagonal rings. In these, Ge1–Ge1 and Ge2–Ge2 dimers are interconnected by two Ni atoms to form hexagonal rings that are stacked and bridged by Ge3 atoms along the *c* axis (Figure 2B). Similar to the Yb2 atoms in the pentagonal tunnels, Yb3 atoms are also sandwiched between the hexagonal rings. The widest channels

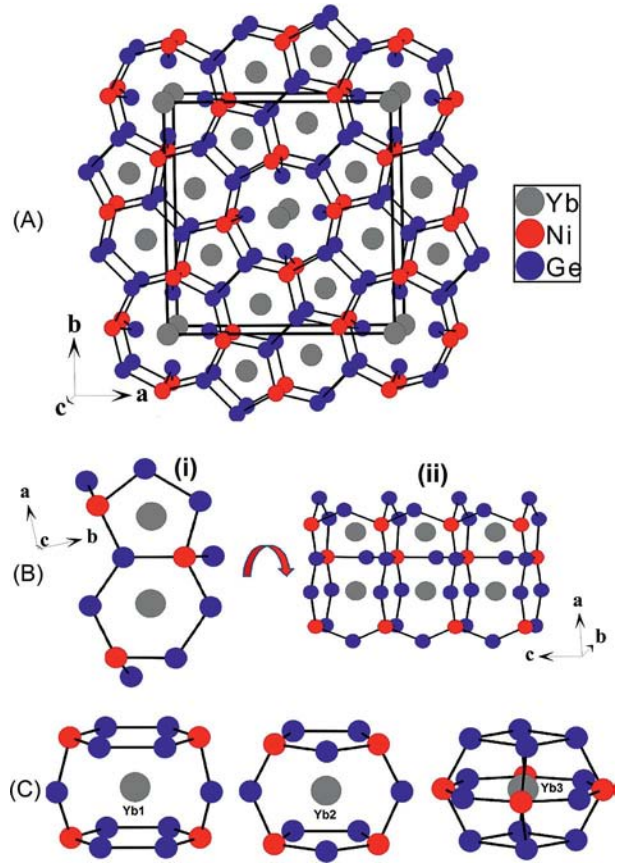

Figure 2. (A) The structure of $Yb_5Ni_4Ge_{10}$ as viewed along the *c* axis; the unit cell is outlined. (B) (i) Projection of hexagonal and pentagonal rings along the *ab* plane, and (ii) their propagation along the *c* axis through Ni–Ge–Ni zigzag chains. (C) Coordination environment for all three Yb atoms in $Yb_5Ni_4Ge_{10}$. No atoms are shown that have bond lengths longer than 3.5 Å.

in the structure are built from stacked alternating planar octagonal and square rings interconnected through Ni–Ge2 and Ge3–Ge3 bonds, in which the octagons are composed of alternating four Ni and four Ge2 atoms, and the square rings are composed of four Ge3 atoms. Yb1 atoms sit in the center of the octagonal rings. The Ge3–Ge3 distance in the square ring can be considered as a weak bonding interaction, because of the large interatomic distance of 2.9162(3) Å. The large Ge–Ge distances were observed in $Yb_5T_4Ge_{10}$ (T = Co, Rh, Ir) compounds as well.[12]

The interlayer Ni–Ge distances [2.3397(4) Å] are shorter and stronger than the intralayer Ni–Ge distance [2.4308(3) Å and 2.3806(3) Å], and all Ni–Ge distances are shorter than the sum of the covalent radii of 2.77 Å[33] which indicates strong Ni–Ge interactions. The Ni–Ge interlayer distances are comparable to 2.327 Å in $YbNiGe_2$,[29] and the Ni–Ge intralayer distances are comparable to 2.428 Å in YbNiGe,[24] 2.404 Å in $YbNi_2Ge_2$,[24] and 2.421 Å $Yb_3Ni_{11}Ge_4$.[24] The Ge1–Ge1 [2.466(3) Å] distances are similar to those in the diamond modification of germanium (2.45 Å).[34]

Crystallographically, there are three different Yb sites in $Yb_5Ni_4Ge_{10}$, and the coordination environment around each (Figure 2C) is significantly different. The Yb1 atom, located at the hexagonal tunnel, is in contact with four Ni atoms and 10 Ge atoms. The Yb2 atom has a coordination with eight Ge and four Ni atoms, whereas the Yb3 atom is surrounded by ten Ge atoms and four Ni atoms. Because of the different size of Yb coordination environment, a wide range for the Yb–Ni distances [2.8470(3)–3.2270(4) Å] and Yb–Ge [2.9820(3)–3.2919(3) Å] is observed. The average distance obtained for Yb3–Ge, 3.1824 Å, is longer than the corresponding distance for Yb1–Ge and Yb2–Ge with 3.0227 and 2.955 Å, respectively. Similarly, the average distance obtained for Yb3–Ni, 3.2919 Å, is also longer than the corresponding distance for Yb1–Ni and Yb2–Ni with 3.1086 and 2.9820 Å, respectively. Considering the possibility of mixed-valent behavior of the ytterbium atoms, as it is evident from the magnetic susceptibility measurements (discussed below), the Yb1 and Yb2 sites appear to be occupied with smaller Yb^{3+} and the Yb3 site with larger Yb^{2+} atoms.

Magnetism

The magnetic susceptibility measurements on $Yb_5Ni_4Ge_{10}$ samples indicate a paramagnetic substance, which reveals the presence of Yb^{3+} species in the structure. In Figure 3 the molar magnetic susceptibility ($\chi_m = M/H$) measured in a field of 5 kOe is shown. No long-range magnetic order could be observed down to 2 K. The susceptibility rises with decreasing temperature as observed for paramagnets. However, the inverse susceptibility (χ_m^{-1}), plotted on the right axis of the Figure 3, shows significant deviation from linearity below 100 K. From the linear region (200–300 K), the calculated value for the paramagnetic Curie temperature (θ_p) is –73.6 K. The relatively large and negative θ_p value indicates predominantly antiferromagnetic coupling between the Yb moments. Another point to notice is the effective Bohr magneton number (μ_{eff}) observed from the linear fit. The observed value of μ_{eff} is 8.1 μ_B per formula unit, which corresponds to 3.6 μ_B/Yb ion. The calculated value of magnetic moment for a free trivalent ytterbium ($4f^{13}$) ion is 4.55 μ_B (for $g = 8/7$, $J = 7/2$, $L = 3$ and $S = 1/2$). However, in light of the crystal chemistry discussed above, which suggests 2/3 of the Yb per formula is trivalent and the rest is divalent, we can consider only three Yb^{3+} ions per formula. In this scenario, the moment value calculated is 4.6 μ_B/Yb ion, which is closer to the expected free ion Yb^{3+} moment. We have also measured the low-field magnetic susceptibility of $Yb_5Ni_4Ge_{10}$ under zero-field-cooled and field-cooled conditions of the sample by applying a field of 100 Oe. The data is plotted as an inset to Figure 3. The absence of any anomaly in $\chi_m(T)$ and ZFC–FC bifurcation rules out any long-range magnetic ordering in this compound as well as any magnetic frustration. In Figure 4, magnetization measured at $T = 2$ and 300 K is plotted as a function of field. At 300 K, M varies linearly with H, indicating a complete paramagnetic state. The low-temperature data also supports the persistent paramagnetic state of the compound, as the data can be fitted to the Brillouin function for Yb^{3+} ($g = 8/7$ and $J = 7/2$).

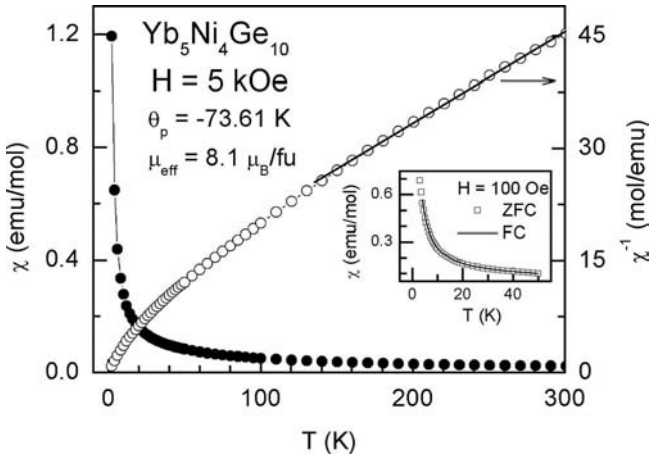

Figure 3. Molar magnetic susceptibility ($\chi = M/H$) for $Yb_5Ni_4Ge_{10}$ measured in a field of 5 kOe. The inverse susceptibility (χ^{-1}) is also plotted. The straight line passing through the data points is the linear fit of the Curie–Weiss law. The paramagnetic Curie temperature (θ_p) and the effective Bohr magneton number (μ_B), calculated from the slope of the Curie–Weiss fit are also shown in the figure The inset shows the low-field ($H = 100$ Oe) susceptibility measurement in the zero-field-cooled (ZFC) and field-cooled (FC) states of the sample.

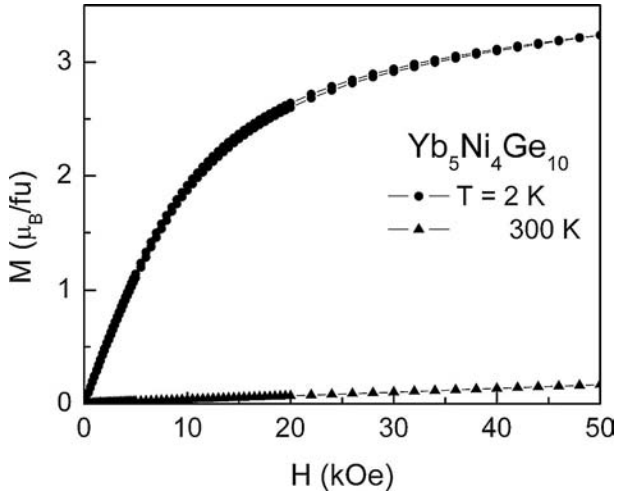

Figure 4. Magnetization (M) measured as a function of field (H) at $T = 2$ and 300 K.

Specific Heat

The absence of long-range magnetic ordering in $Yb_5Ni_4Ge_{10}$ was already observed from the magnetic susceptibility measurements. Further evidence for this can be found in the plot of specific heat, (C) shown in Figure 5. C decreases as the temperature is lowered. $C(T)$ does not exhibit any anomaly, thus ruling out any type of long-range phase transitions. $C(T)$ has been shown in different forms

as insets in Figure 5. The observed specific heat at low temperatures can be described by the equation $C = \gamma T + \beta T^3$, which describes that the total specific heat of the sample comprises the contributions from the electronic part (coefficient of electronic specific heat, γ) and the lattice part (β). Thus, at low temperatures C should vary as a function of T^3, that is, the plot of C/T vs. T^2 should be a straight line.[35] Such a plot is convenient for calculating the values of both γ and β.

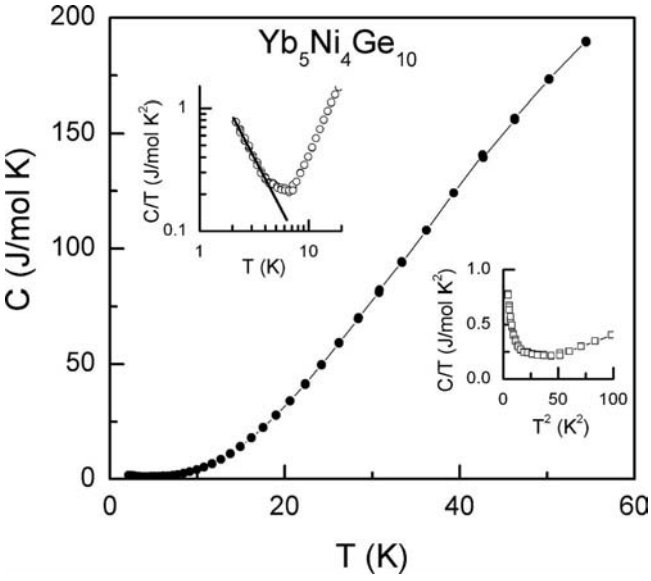

Figure 5. Specific heat (C) measured as a function of temperature for $Yb_5Ni_4Ge_{10}$. The insets exhibit the variation of C/T as a function of T (left-top inset, data plotted on log scale) and T^2 (right-bottom inset). A straight line is drawn through the data points in the left-top inset to highlight the linear variation of C/T with respect to T at temperatures below 5 K, to show the possibility of non-Fermi-liquid-like behavior in $Yb_5Ni_4Ge_{10}$.

However, it is quite intriguing to observe that C/T does not vary linearly with T^2, and at low temperatures (below 5 K) there is a clear upturn. On a log-scale, there is a linear variation of this upturn as a function of T as shown by the straight line passing through the data points in the top inset in Figure 5. This observation along with the absence of a long-range magnetic order in magnetic susceptibility fulfills two of the three signatures for a non-Fermi-liquid-like behavior in this compound below 5 K.[36] Another interesting point to observe is the behavior of $C(T)$ at temperatures between 5 and 10 K. In this region, the heat capacity neither varies linearly with T nor does it decrease as a function of T. It appears as if the system enters the non-Fermi-liquid state via an intermediate state. More calorimetric, transport, and structural experiments are required to probe this interesting behavior of $Yb_5Ni_4Ge_{10}$ in detail.

Concluding Remarks

The new compound $Yb_5Ni_4Ge_{10}$ was obtained from reactions in molten In over a broad range of synthetic conditions. The flux method proves to be an excellent tool for discovering new intermetallic compounds with complex crystal structures. The room-temperature structure ($Sc_5Co_4Si_{10}$ type) was refined from single-crystal X-ray diffraction data. The magnetization data exhibits absence of long-range magnetic interaction; however, short-range magnetic correlations do exist in the system. The specific heat measurements exhibit signatures of a non-Fermi-liquid-like behavior below 5 K. It is expected that band-structure calculations on this compound might yield important information regarding the electronic structure and its influence on the physical properties. Systematic temperature and magnetic-field-dependent structural, thermal, transport, and magnetic measurements of $Yb_5Ni_4Ge_{10}$ will bring out the underlying physical phenomenon.

Experimental Section

Reagents: The following reagents were used as purchased without further purification: Yb (in the form of powder ground from the metal lump, 99.99% HEFA Rare Earth Canada Co. Ltd), Ni (ca. 200 mesh, 99.95% Cerac, Milwaukee, WI), Ge (ca. 100 mesh, 99.999% Cerac, Milwaukee, WI), and In (tear drops 99.99% Plasmaterials, Livermore, CA).

Synthesis: $Yb_5Ni_4Ge_{10}$ was obtained by combining ytterbium metal (0.3 g, 5 mmol), nickel (0.08 g, 4 mmol), germanium (0.26 g, 10 mmol), and indium (1.79 g, 45 mmol) in an alumina crucible under an inert nitrogen atmosphere inside a glove box. The crucible was placed in a 13 mm fused silica tube, which was flame-sealed under a vacuum of 10^{-4} Torr, to prevent oxidation during heating. The reactants were then heated to 1000 °C over 10 h, maintained at that temperature for 5 h to allow proper homogenization, then cooled to 850 °C in 2 h and kept at this temperature for 48 h. Finally, the sample was allowed to slowly cool to 50 °C over 48 h. The reaction product was isolated from the excess indium flux by heating at 350 °C and subsequently centrifuging through a coarse frit. Any remaining flux was removed by immersion and sonication in glacial acetic acid for 48 h. The final crystalline product was rinsed with water and dried with acetone. This method produced the target compound with ca. 99% purity and in a yield more than 95% on the basis of the initial amount of Yb metal used in the reaction. Main side products were very small amounts of recrystallized Ge and residual In metal flux. Rod-shaped crystals, often aggregated in bundles, of $Yb_5Ni_4Ge_{10}$, which grow as metallic silvery rods, were carefully selected for elemental analysis, structure characterization, and physical property measurements.

Elemental Analysis: Semi-quantitative microprobe analyses of the samples were performed with a Hitachi S-3400 scanning electron microscope (SEM) equipped with a PGT energy dispersive X-ray analyzer. Data were acquired with an accelerating voltage of 20 kV and in 60 s accumulation time. The EDS analysis performed on visibly clean surfaces of the samples indicated that the atomic composition was close to 5:4:10.

Powder X-ray Diffraction: Phase identity and purity of the $Yb_5Ni_4Ge_{10}$ sample was determined by powder XRD experiments that were carried out with an Inel diffractometer by using Cu-K_α radiation. The experimental powder pattern was compared to patterns calculated from the single-crystal X-ray structure refinement.

Single-Crystal X-ray Diffraction: The X-ray intensity data of $Yb_5Ni_4Ge_{10}$ were collected at room temperature by using a STOE IPDS 2T (with additional capability of 2θ swing of the detector)

diffractometer with graphite-monochromatized Mo-K_α (λ = 0.71073 Å) radiation. The X-AREA (X-RED and X-SHAPE within) package suite[31] was used for the data extraction and integration and to apply numerical absorption corrections. Details of the crystallographic data are given in Table 1.

Table 1. Crystal data and structure refinement for $Yb_5Ni_4Ge_{10}$.

Empirical formula	$Yb_5Ni_4Ge_{10}$
Formula weight	1826.06
Temperature (K)	293(2)
Wavelength (Å)	0.71073
Crystal system	Tetragonal
Space group	*P*4/*mbm*
Unit cell dimensions	
a (Å)	12.6716(18)
b (Å)	12.6716(18)
c (Å)	4.1598(8)
α (°)	90.00
β (°)	90.00
γ (°)	90.00
Volume (Å^3)	667.94(19)
Z	2
Calculated density (g/cm^3)	9.079
Absorption coefficient (mm^{-1})	62.156
F(000)	1563
Crystal size (mm^3)	0.12 × 0.08 × 0.08
θ range for data collection (°)	3.22 to 29.14
Index ranges	$-17 \le h \le 17$, $-17 \le k \le 17$, $-5 \le l \le 5$
Reflections collected	5926
Independent reflections	542 [R_{int} = 0.0668]
Completeness to θ = 29.14°	99.8%
Refinement method	Full-matrix least-squares on F^2
Data/restraints/parameters	542/0/34
Goodness-of-fit	1.279
Final R[a] indices [$>2\sigma(I)$]	R_{obs} = 0.0302, wR_{obs} = 0.0430
R indices [all data]	R_{all} = 0.0365, wR_{all} = 0.0441
Extinction coefficient	0.0075(2)
Largest diff. peak and hole (e Å^{-3})	1.764 and –1.782

[a] $R = \Sigma||F_o| - |F_c||/\Sigma|F_o|$, $wR = \{\Sigma[w(|F_o|^2 - |F_c|^2)^2]/\Sigma[w(|F_o|^4)]\}^{1/2}$ and calcd. $w = 1/[\sigma^2(F_o^2) + (0.0095P)^2 + 8.8012P]$ where $P = (F_o^2 + 2F_c^2)/3$.

The room-temperature data set of $Yb_5Ni_4Ge_{10}$ was compatible with space group *P*4/*mbm*. The atomic parameters of $Sc_5Co_4Si_{10}$ were then taken as starting values, and the structure was refined with SHELXL–97 (full-matrix least-squares on F^2)[32] with anisotropic atomic displacement parameters for all atoms. Refinement of the occupancy parameters showed full occupancy within two standard deviations. The final difference electron-density synthesis was flat. The results of the structure refinement are summarized in Table 1. The atomic coordinates and the anisotropic displacement parameters are listed in Tables 2 and 3. Group bond lengths with estimated standard deviations are listed in Table 4.

Table 2. Atomic coordinates (× 10^4) and equivalent isotropic displacement parameters (Å^2 × 10^3) for $Yb_5Ni_4Ge_{10}$ at 293(2) K with estimated standard deviations in parentheses.

Label	Wyckoff site	*x*	*y*	*z*	Occupancy	U_{eq}[a]
Yb1	4*h*	0	0	0	1	4(1)
Yb2	4*h*	3227(1)	8227 (1)	5000	1	4(1)
Yb3	2*a*	3902(1)	1098(1)	5000	1	5(1)
Ni	8*i*	2437(1)	9717(1)	0	1	4(1)
Ge1	4*g*	4312(1)	9312(1)	0	1	4(1)
Ge2	8*i*	2008(1)	1546(1)	0	1	7(1)
Ge3	8*j*	5040(1)	3373(1)	5000	1	7(1)

[a] U_{eq} is defined as one third of the trace of the orthogonalized U_{ij} tensor.

Table 3. Anisotropic displacement parameters (Å^2 × 10^3) for $Yb_5Ni_4Ge_{10}$ at 293(2) K with estimated standard deviations in parentheses.[a]

Label	U_{11}	U_{22}	U_{33}	U_{12}	U_{13}	U_{23}
Yb1	4(1)	4(1)	5(1)	0	0	0
Yb2	4(1)	4(1)	4(1)	–1(1)	0	0
Yb3	5(1)	5(1)	7(1)	0(1)	0	0
Ni	3(1)	2(1)	5(1)	0(1)	0	0
Ge1	2(1)	2(1)	7(1)	–1(1)	0	0
Ge2	4(1)	2(1)	14(1)	1(1)	0	0
Ge3	14(1)	4(1)	4(1)	3(1)	0	0

[a] The anisotropic displacement factor exponent takes the form: $-2\pi^2[h^2a^{*2}U_{11} + ... + 2hka^*b^*U_{12}]$.

Table 4. Grouped bond lengths (Å) for $Yb_5Ni_4Ge_{10}$ at 293(2) K with estimated standard deviations in parentheses.

Label	Distance	Label	Distance
Yb1–Ge3 × 8	2.9287(8)	Yb3–Ni1 × 2	3.2916(11)
Yb1–Ni × 4	3.1087(13)	Ni–Ge3 × 2	2.3398(8)
Yb2–Ge1 × 2	2.8470(11)	Ni–Ge2	2.3802(17)
Yb2–Ni × 4	2.9822(10)	Ni–Ge1	2.4308(15)
Yb2–Ge3 × 2	2.9888(12)	Ni–Ge2	2.4599(17)
Yb2–Ge2 × 4	2.9921(9)	Ge1–Ge1	2.466(3)
Yb3–Ge1 × 4	3.1171(8)	Ge2–Ge2	2.593(2)
Yb3–Ge3 × 2	3.2241(12)	Ge2–Ge3 × 2	2.9323(12)
Yb3–Ge2 × 4	3.2269(10)	Ge3–Ge3 × 2	2.9159(16)

Further details of the crystal structure investigations may be obtained from the Fachinformationszentrum Karlsruhe, 76344 Eggenstein-Leopoldshafen, Germany [Fax: (+49)7247-808-666; E-mail: crysdata@fiz-karlsruhe.de] on quoting the depository number CSD-422876 for $Yb_5Ni_4Ge_{10}$.

Magnetization and Specific Heat Measurements

Magnetic measurements of $Yb_5Ni_4Ge_{10}$ as a function of temperature (magnetic susceptibility) and field (magnetization) were carried out with a Quantum Design made MPMS-SQUID magnetometer at TIFR-Mumbai, India.

Heat capacity was measured with a Quantum Design Physical Properties Measurement System (PPMS). An addendum was first collected on the sample puck containing a small amount of Apiezon N grease from 50–2 K for background subtraction. Several single crystals of $Yb_5Ni_4Ge_{10}$ (4.6 mg) were then mounted and measured under zero applied field within the same temperature range.

Acknowledgments

Financial support from the Department of Energy (Grant DE-FG02-07ER46356) is gratefully acknowledged. S. R. is thankful to Ganesh S. Jangam, and Kartik K. Iyer for magnetic measurements.

[1] H. F. Braun, K. Yvon, R. M. Braun, *Acta Crystallogr., Sect. B-Struct. Science* **1980**, *36*, 2397.
[2] N. G. Patil, S. Ramakrishnan, *Physica B: Condensed Matter* **1997**, *237–238*, 594.
[3] N. G. Patil, S. Ramakrishnan, *Phys. Rev. B* **1997**, *56*, 3360.

[4] M. Kolenda, M. Hofmann, J. Leciejewicz, B. Penc, A. Szytula, *Appl. Phys. A* **2002**, *74*, S769.
[5] L. S. Hausermannberg, R. N. Shelton, *Phys. Rev. B* **1987**, *35*, 6659.
[6] H. F. Braun, C. U. Segre, *Solid State Commun.* **1980**, *35*, 735.
[7] B. Kindler, D. Finsterbusch, R. Graf, F. Ritter, *Phys. Rev. B* **1994**, *50*, 704.
[8] E. Bauer, *Adv. Phys.* **1991**, *40*, 417.
[9] P. Wachter, *Handbook on the Physics and Chemistry of Rare Earths*, Elsevier Science, Amsterdam, **1994**, p. 177.
[10] J. M. Lawrence, P. S. Riseborough, R. D. Park, *Rep. Prog. Phys.* **1981**, *44*, 1.
[11] Z. Fisk, D. W. Hess, C. J. Pethick, D. Pines, J. L. Smith, J. D. Thomson, J. O. Willis, *Science* **1988**, *239*, 33.
[12] K. Katoh, T. Tsutsumi, K. Yamada, G. Terui, Y. Niide, A. Ochiai, *Physica B: Condensed Matter* **2006**, *373*, 111.
[13] Z. Hossain, M. Schmidt, W. Schnelle, H. S. Jeevan, C. Geibel, S. Ramakrishnan, J. A. Mydosh, Y. Grin, *Phys. Rev. B* **2005**, *71*, 060406.
[14] M. Chondroudi, M. Balasubramanian, U. Welp, W. K. Kwok, M. G. Kanatzidis, *Chem. Mater.* **2007**, *19*, 4769.
[15] M. A. Zhuravleva, M. G. Kanatzidis, *J. J. Solid State Chem.* **2003**, *173*, 280.
[16] M. A. Zhuravleva, J. Salvador, D. Bilc, S. D. Mahanti, J. Ireland, C. R. Kannewurf, M. G. Kanatzidis, *Chem. Eur. J.* **2004**, *10*, 3197.
[17] C. P. Sebastian, J. Salvador, J. B. Martin, M. G. Kanatzidis, *Inorg. Chem.* **2010**, *49*, 10468.
[18] C. P. Sebastian, M. G. Kanatzidis, *J. J. Solid State Chem.* **2010**, *183*, 2077.
[19] S. Margadonna, K. Prassides, M. Chondroudi, J. R. Salvador, M. G. Kanatzidis, *Chem. Commun.* **2005**, 5754.
[20] X. N. Wu, M. Francisco, Z. Rak, T. Bakas, S. D. Mahanti, M. G. Kanatzidis, *J. J. Solid State Chem.* **2008**, *181*, 3269.
[21] M. Chondroudi, S. C. Peter, C. D. Malliakas, M. Balasubramanian, Q. Li, M. G. Kanatzidis, *Inorg. Chem.* **2011**, *50*, 1184.
[22] W. Rieger, E. Parthe, *Monatsh. Chem.* **1969**, *100*, 444.
[23] Y. K. Gorelenko, P. K. Starodub, V. A. Bruskov, R. V. Skolozdra, V. I. Yarovetz, O. I. Bodak, V. K. Pecharsky, *Ukrainskii. Fizicheskii. Zh.* **1984**, *29*, 867.
[24] R. B. Dzyanyi, O. I. Bodak, V. B. Pavlyuk, *Russ. Metall.* **1995**, 133.
[25] H. S. Jeevan, Z. Hossain, C. Geibel, *Physica B: Condensed Matter* **2005**, *359*, 235.
[26] K. Shigetoh, D. Hirata, M. A. Avila, I. Takabatake, *J. Alloys Compd.* **2005**, *403*, 15.
[27] K. Grube, T. Wolf, P. Adelmann, C. Meingast, H. Von Lohneysen, *Physica B: Condensed Matter* **2006**, *378–80*, 750.
[28] K. Umeo, N. Hosogi, M. A. Avila, T. Takabatake, *Phys. Status Solidi B* **2010**, *247*, 751.
[29] J. R. Salvador, J. R. Gour, D. Bilc, S. D. Mahanti, M. G. Kanatzidis, *Inorg. Chem.* **2004**, *43*, 1403.
[30] M. G. Kanatzidis, R. Pottgen, W. Jeitschko, *Angew. Chem. Int. Ed.* **2005**, *44*, 6996.
[31] *X-AREA*, Stoe & Cie GmbH, Darmstadt, **2006**.
[32] *SHELXTL*, 5.10 ed., Bruker Analytical X-ray Systems, Inc., Madison, WI, **1998**.
[33] J. Emsley, *The Elements*, Clarendon Press, Oxford, **1989**.
[34] J. Donohue, *The Structures of the Elements*, Wiley, New York, **1974**.
[35] E. S. R. Gopal, *Specific Heat at Low Temperatures*, Plenum, New York, **1966**.
[36] G. R. Stewart, *Rev. Mod. Phys.* **2001**, *73*, 797.

Received: April 1, 2011
Published Online: June 6, 2011

